

# MODEL REFERENCE ADAPTIVE CONTROL IN DISCRETE-TIME APPLIED ON THE LLC LED DRIVER

MAIKEL F. MENKE\*, RODRIGO V. TAMBARA\*, ÁLYSSON RANIERE SEIDEL\*

\*Federal University of Santa Maria

Electrical and Computational Systems Research and Development Group - GSEC/CTISM  
Santa Maria, Rio Grande do Sul, Brazil

Emails: maikelmanke@gmail.com, rodvarella10@gmail.com, seidel@ctism.ufsm.br

**Abstract**— This paper presents the model reference adaptive control (MRAC) applied to the DC/DC LLC resonant converter supplying a light emitting diode (LED) based load. The MRAC is employed in order to overcome the drawback of closed-loop control system with changeable controller gains, which are needed to obtain a good performance at different operating points of the converter. The MRAC is designed to maintain the average LED current controlled at the reference value, which will be changed to obtain LED current amplitude modulation, consequently dimming. Furthermore, to avoid LED current modulating, raised from the unavoidable bus voltage ripple in an off-line LED driver, the adaptive controller algorithm measures the bus voltage ripple and changes the control action to attenuate its effect on the output LED current. Experimental results shows the feasibility of adaptive control applied to the LED driver.

**Keywords**— Active Ripple Compensation, Adaptive Control, Digital Control, LED Driver, LLC, Resonant Converter.

## 1 INTRODUCTION

Artificial lighting systems are widely discussed in the literature, being currently LED based lamps the most efficient, flexible, and reliable light source (Almeida et al., 2015), (Branas et al., 2013). Unlike of discharge lamps, LED based lamps have to be supplied by a controlled current source, due to the direct relationship between the LED output light and its forward current, combined with a dynamic high bandwidth of the LED output light (Schratz et al., 2016).

Considering the electronic circuit designed to supply an LED load, known as LED driver, usually PWM and resonant converters are employed. Concerned with the efficiency of the system, resonant converters are becoming more popular on LED driver due to their higher efficiency and power density when compared to PWM converters (Wu, 2011).

An usual structure of the off-line LED driver designed to supply a medium to high power (>70 W) is shown in Figure 1. Functionalities as dimming capability and universal input voltage operation are commonly and easily incorporated in this structure (Almeida et al., 2015). As can be seen, two stages compose the LED driver. The power factor correction (PFC) stage defines the consumed power quality, providing a high power factor and reduced current harmonic injection into the line. Besides, for universal input voltage systems, the PFC stage has to control the average bus voltage ( $V_{BUS}$ ) in a fixed value or inside a predefined range. The second stage, usually referred to as power control (PC) stage, is strictly responsible to control the LED current ( $i_{LED}$ ). In addition, it has to provide an LED current with reduced ripple to avoid flicker, which amplitude should follow the IEEE 1789-2015 recommended practice (IEEE Power Electronics Society, 2015).

Concerned with the LED driver reliability, special attention has been given to the DC-link capacitance, where electrolytic capacitors (E-Cap) are being

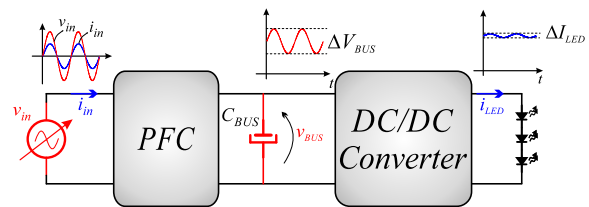


Figure 1 Off-line two stage LED driver structure diagram.

substituted by film capacitors (F-Cap), which presents longer lifetime with the drawback of lower energy density (Almeida et al., 2015), (Ma et al., 2011). To overcome the issue of a reduced energy density, it is allowed to the DC-link implemented with F-Cap to present a lower capacitance, thus avoiding the increase of the driver volume. However, a higher bus voltage ripple ( $\Delta V_{BUS}$ ) in low frequency (LF) (double of the input line) is unavoidable. In order to avoid the system functioning deterioration, the PC stage has to both maintain an average LED current controlled and attenuate the LF LED current ripple ( $\Delta I_{LED}$ ), which is excited by  $\Delta V_{BUS}$ .

Currently, a research topic that is receiving considerable attention on LED driver is the control system design, specially for the PC stage. Being the main challenge to design a control system that is capable of maintaining an average LED current controlled, attenuate LF current ripple and provide a good overall dynamic performance of the driver simultaneously (Soares et al., 2017). The  $\Delta I_{LED}$  reduction technique through the control system is known in the literature as active ripple compensation (ARC). Since this solution bypass the need of significant hardware changes, it is likely one of the most suitable approach to overcome this issue.

To employ classical control techniques to design specifically the feedback compensator of the PC stage, the control-to-output transfer function (TF) has to be known for each steady-state operating point, which will change as function of the average bus voltage and

average LED current. Thus, the control system design becomes a hard task, where the interest TF has to be obtained for all operating points and for each condition a proper compensator has to be designed. As a result, the control system has to identify the current operating condition and select the proper compensator gain from a lookup table.

As an alternative, in this paper the adaptive control technique will be investigated and employed to control the LED driver. The adaptive control is justified in this work due to uncertainty on the model of the plant during the LED dimming, input voltage variation and unavoidable parametric variations. In other words, under dimming operating the plant dynamic changes, becoming unknown. However, due to the nature operation of the adaptive controller, the compensator gains will change automatically in order to obtain a good performance over a wide operation area. In this way, it is not necessary to work with lookup tables, besides, it is not any more necessary to design the controller gains for each operating point of the converter.

The remaining of this paper is organized as follows. Section II presents the LLC DC/DC converter employed to feed an LED-based load. Section III deals with the adaptive control design for the LLC LED driver. Experimental results are shown in section IV, being the conclusions of this paper presented on section V.

## 2 LLC LED DRIVER

Figure 2 shows the schematic diagram of the DC/DC LLC resonant converter supplying an LED-based load, which will be referred as LLC LED driver. As it can be seen, this stage is composed by a half-bridge (HB) inverter ( $S_1$  and  $S_2$ ), LLC resonant filter ( $L_S$ ,  $C_S$ ,  $L_M$ ), transformer ( $n_P$ ,  $n_{S1}$ ,  $n_{S2}$ ), output rectifier ( $D_1$ ,  $D_2$ ), and output low pass filter ( $C_O$ ).

In order to implement the second stage, the use of the LLC resonant converter is becoming usual (Wu, 2011), (Wang et al., 2016), due to their wide operation range and high efficiency in all conditions, presenting more advantages over others topologies. However, although the LLC have been widely used in LED drivers, its small-signal model and a proper feedback compensator designed to ARC have not been completely reported. Focusing on evaluate the adaptive control for the LLC LED driver, this paper follows neglecting the PFC analysis and design, being the bus voltage emulated by a controlled voltage power source.

In the LLC LED driver, when the HB switching frequency ( $f_{sw}$ ) changes, the LED forward current changes as function of the LED and LLC converter parameters. To avoid imprecision in considering the LED as an equivalent resistance, the LLC LED driver is massively investigated in (Wu, 2011), where the non-linear V-I characteristic of the LED is considered to obtain the converter current gain curve. Furthermore, the LLC LED driver design methodology is

also presented in (Wu, 2011), which is based on the derived current and voltage gain curves.

Following the LLC LED driver designed methodology proposed in (Wu, 2011), the LLC resonant filter is designed to supply a 100 W LED module, which load is composed by three chips on board (COB) LEDs connected in series, being the LED non-linear V-I characteristic modeled by the piece-wise linear model (Lin et al., 2013). The parameters are:  $V_{th} = 26.74V$  and  $r_d = 2.073 \Omega$ . To maintain the objectivity, design methodology of the LLC LED driver is omitted, since it is not the contribution of this paper. Table 1 shows the design parameters as well the designed components of the LLC LED driver.

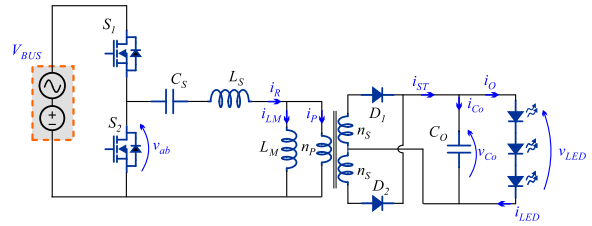


Figure 2 Schematic of the DC/DC LLC resonant converter supplying an LED based load.

Table 1  
LLC LED driver parameters

Parameters	Value
Half-bridge input voltage ( $V_{BUS}$ )	400 V
Half-bridge switching frequency ( $f_{sw}$ )	102.7 kHz
Average output voltage ( $V_{LED}$ )	87.37 V
Average output current ( $I_{LED}$ )	1.15 A
<b>Designed LLC resonant filter</b>	
$C_S$ Resonant capacitor	12 nF
$L_S$ Resonant inductor	200 $\mu$ F
$L_M$ Magnetizing inductance	600 $\mu$ H
$C_O$ Output capacitor (Film capacitor)	10 $\mu$ F/100V
$N_P/N_S$ Transformer turns ratio (n)	2.28
	EE 30/15/14; $n_P=44 - 2xAWG26$ ; $n_S=17 - 3xAWG26$

## 3 MODEL REFERENCE ADAPTIVE LED CURRENT CONTROL

As an alternative to the classical controllers, the model reference adaptive control (MRAC) technique is employed in this paper to control the LLC LED driver. The MRAC technique is selected due to the capability in easily defining the converter closed loop performance through the model reference.

### 3.1 Plant Modelling

In order to obtain a discrete-time mathematical model of the plant, needed to design the MRAC controller, the following analysis is developed. Initially consider the SISO (Single input Single output) plant in discrete-time given by (1).

$$\frac{y(z)}{u(z)} = G(z) = G_p(z)(1 + \mu\Delta_m(z)) + \mu\Delta_a(z) \quad (1)$$

Which  $G_p(z)$  represents the modeled part of the plant;  $\mu\Delta_m(z)$  and  $\mu\Delta_a(z)$  are the unmodeled dynamics of multiplicative and additive types, respectively; and  $y(z)$  (in this case,  $I_{LED}$ ) is the plant output and  $u(z)$  is the plant input.

The modelled part of the plant is given by (2).

$$G_p(z) = k_p \frac{Z_p(z)}{R_p(z)} \quad (2)$$

Which  $Z_p(z)$  and  $R_p(z)$  are monic polynomials of degree  $m_p$  and  $n_p$ , respectively;  $Z_p(z)$  is a Schur polynomial and the signal of  $k_p$  is assumed to be known.

In relation to the unmodelled dynamics, the following assumptions are made:

**A1:**  $\Delta_a(z)$  is a strictly proper and Schur TF;

**A2:**  $\Delta_m(z)$  is a Schur TF;

**A3:** The only *a priori* information required about  $\Delta_a(z)$  and  $\Delta_m(z)$  is a lower bound on the stability margin  $p$  of its poles.

### 3.2 Discrete-time nominal model of the plant

To start with the MRAC analysis, it is necessary to have a brief insight about the plant dynamic behavior. Thus, to obtain the LLC DC/DC resonant converter small-signal model, the extended describing function (EDF) method is employed (Yang et al., 1992), (Chang et al., 2012). Applying the EDF method to obtain the control-to-output transfer function of the LLC LED driver and using the parameters given on Table 1 results in a seventh-order function. Neglecting poles and zeros higher than the  $f_{sw}$ , a nominal fourth-order system is obtained, given by (3).

$$\frac{\hat{i}_O}{\hat{f}_{SN}} = \frac{\hat{i}_{LED}}{\hat{f}_{SN}} = G_p(s) = \frac{4.2947 \cdot 10^{15} (s - 5.878 \cdot 10^5)}{(s^2 + 1.611 \cdot 10^4 s + 1.051 \cdot 10^9)(s^2 + 1.353 \cdot 10^5 s + 2.566 \cdot 10^{11})} \quad (3)$$

Which  $\hat{i}_{LED}$  is the output current (controlled variable  $y$ ) and  $\hat{f}_{sn}$  is the normalized  $f_{sw}$  (control action  $u$ ).

However, due to the variation of the operating point, as well as a parametric variation, the dynamic behavior of the LLC LED driver changes. In the classical control system design, the converter dynamic in each operating point is analyzed and the compensator gains are tuned to properly control the system in this condition. In practice, the compensator is composed by a lookup-table, where the control system has to select the correct gain from this table as a function of the operating point. Nevertheless, since the small-signal modeling procedures of the LLC LED driver are based on the FHA, its accuracy is diminished in operating points away from the main resonance (Menke et al., 2018). Thus, even designing an optimal classical controller for several operating points, the controller performance will differ from the expected behavior since the employed model does not correspond to the real converter dynamic behavior. To overcome this issues, the MRAC will be used, where the controller gains are calculated based on an expected out-

put performance, given by the reference model of the controller.

In order to simplify the MRAC control, the LLC dynamic behavior for the nominal operating point will be represented through a reduced order TF, being neglected the high frequency dynamics. This practice is usual during the MRAC design, since it presents a high robustness against unmodelled dynamics of the converter. Thus, to obtain a nominal model for the plant, a second-order small-signal approximation for the LLC LED driver is used, given by (4).

$$G_p(s) = \frac{K}{(s^2 + as + b)} \quad (4)$$

For the converter nominal operating point, the LLC LED driver second-order approximation is given by (5).

$$G_p(s) = \frac{-9.8680 \cdot 10^9}{(s^2 + 1.617 \cdot 10^4 s + 1.054 \cdot 10^9)} \quad (5)$$

Using a zero-order-hold (ZOH) with sampling frequency ( $f_{sa}$ ) of 40 kHz, the discrete time nominal model of the plant is obtained, shown on (6).

$$G_p(z) = \frac{-2.566z - 2.236}{z^2 - 1.155z + 0.6676} \quad (6)$$

Figure (3) shows the Bode Diagram for the different approximations of the LLC LED driver dynamics, where it can be seen that the simplifications adopted do not compromise the analysis, since the LLC LED driver dynamic does not differ considerable from the different approximation at low frequency (< 7kHz).

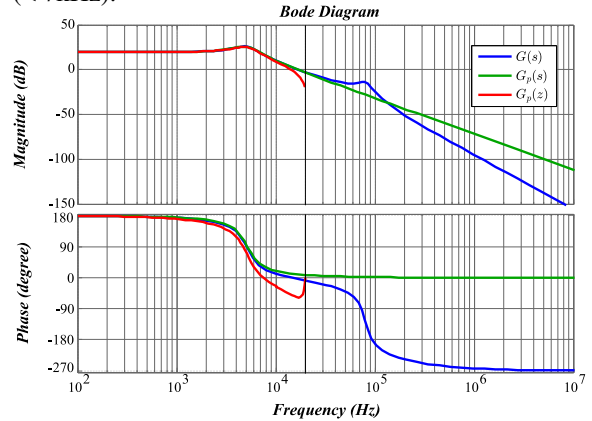


Figure 3 LLC LED driver Bode diagram for different approximations.

### 3.3 Adaptive control strategy

The purpose of the MRAC is to determine the parameters of the controller, such that the closed loop system output ( $y$ ) behave as close as possible of the pre-determined reference model output ( $y_m$ ), represented by the transfer function  $W_m(z)$  (Ioannou and Tsakalis, 1986) and (Massing et al., 2012), defined by (7).

$$W_m(z) = \frac{y_m(z)}{r(z)} = k_m \frac{Z_m(z)}{R_m(z)} \quad (7)$$

Which  $Z_m(z)$  and  $R_m(z)$  are arbitrary Schur monic polynomials (Ioannou and Tsakalis, 1986). The input of  $W_m(z)$  is defined by the reference  $r$ , an uniformly bounded signal. The outcome of (7) is used to generate the signal  $y_m$ , which is the desired value of  $y$  ( $I_{LED}$ ). In the ideal case,  $\mu = 0$  in (1), the perfect tracking can be achieved, it means  $y_m = y$ . Since (6) has relative degree  $n^* = 1$ , (7) can be written as a second-order transfer function with relative degree  $n^* = 1$ , given by (8).

$$W_m(z) = \frac{0.023996(z + 0.7581)}{(z - 0.9230)(z - 0.4724)} \quad (8)$$

The next step is to define the control action, which is given by (9).

$$u(k) = \frac{-1}{\theta_u(k)} [\theta_{\omega_1}(k)\omega_1(k) + \theta_{\omega_2}(k)\omega_2(k) + \theta_y(k)y(k) + \theta_{v_b}(k)v_b(k) + r(k)] \quad (9)$$

Which  $\theta^T(k)$  is the parameter vector given in (10),  $y(k)$  is the feedback variable vector,  $u(k)$  is the control action,  $r(k)$  is the reference signal,  $\omega_1(k)$  and  $\omega_2(k)$  are internal filters outputs, and  $v_b(k)$  is the AC component of the bus voltage.

$$\theta^T(k) = [\theta_{\omega_1}(k) \quad \theta_{\omega_2}(k) \quad \theta_y(k) \quad \theta_u(k) \quad \theta_{v_b}(k)] \quad (10)$$

The parametric adaption algorithm is given by (11).

$$\theta(k+1) = \theta(k) - \alpha \frac{\Gamma \zeta^T(k) \varepsilon(k)}{m^2(k)} \quad (11)$$

Which  $\alpha$  and  $\Gamma$  are design constants, and  $\varepsilon(k)$  is the augmented error expressed by (12).

$$\varepsilon(k) = y(k) + \theta^T(k) \zeta(k) \quad (12)$$

Which  $\zeta(k) = W_m(z)\omega(k)$  is an auxiliary vector and  $\omega^T(k) = [\omega_1(k) \quad \omega_2(k) \quad y(k) \quad u(k) \quad v_b(k)]$ . The normalized function  $m^2(k)$  is expressed by (13).

$$m^2(k) = 1 + \zeta^T(k) \Gamma \zeta(k) \quad (13)$$

The adaptive control block diagram is shown in Figure 4. As it can be seen, the bus voltage is measured and its AC component is extracted by a band pass filter (BPF) and linked to MRAC controller. Thus, the product  $\theta_{v_b}(k)v_b(k)$  correspond to the control action portion responsible for the ARC. This parameters are added to the traditional MRAC controller in order to achieve ARC, attenuating the bus voltage ripple transmission to the LED current, allowing the use of long lifetime F-Cap.

### 3.4 Controller parameters

The controller parameters design consists basically in defining the initial conditions for the controller gains of the adaptive scheme, e.g.,  $\theta^T(0)$ , and the parameters  $\Gamma$  and  $\alpha$ . Table 2 shows the employed MRAC parameters. These parameters were chosen after successive simulations and experimental results.

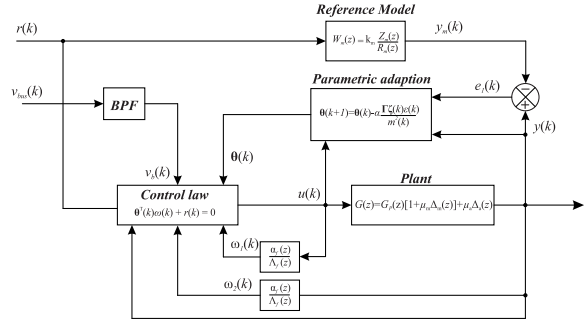


Figure 4 Block diagram of the adaptive controller.

Table 2  
MRAC parameters

Parameter	Values
$\theta^T$	Initial values [0.083536 -0.7325 -0.12662 22.96 -0.07]
$\zeta^T$	Auxiliary vector [0 0 0 0 0]
$\Gamma$	Adaption Matrix $500 * I_{5 \times 5}$
$\alpha$	Scalar design 4000

## 4 EXPERIMENTAL RESULTS

To evaluate the feasibility of the adaptive control applied to the LLC LED driver, experimental results are presented in this section for different operating points. The experimental results are developed for the LLC LED driver with parameters shown in Table 1. IRF840 is used for  $S_1$  and  $S_2$ , and MUR620 for  $D_1$  and  $D_2$ . To implement the MRAC by a digital way, the MCU TM4C1294NCPDT from Texas Instruments is used, which presents a 120 MHz clock and 12 bits ADC converters (Texas Instruments, 2014). To emulate the PFC stage a controllable voltage source is used, being its output set to provide a 400 V average bus voltage plus an AC component at 120 Hz with an amplitude which is function of the dimming level.

Figure 5 shows the LED current, bus voltage and AC component of the LED current for the nominal condition, where the LED current reference is 1.15 A and the bus voltage presents a 42.22 V peak-to-peak ripple. With the same bus voltage ripple and the LLC convert operating in open loop, the LED current presents a ripple of 121%. However, as it can be seen in Figure 5, the LLC LED driver operating in a closed loop with the adaptive control presents a reduced ripple at 120 Hz, being around 16.7%.

Figure 6 shows the LED current, bus voltage and AC component of the LED current for the minimal output power, where the LED current reference is 250 mA and the bus voltage presents a 10.33 V peak-to-peak ripple. The variable bus voltage ripple as function of the dimming level will emulate the real conditions when the bus voltage is provided by the front-end PFC stage. Once, for the maximum output power the ripple will be higher. As function of the LED current reduction, the bus voltage will also reduce. As it can be seen in Figure 6, there is not a noticeable LED cur-

rent ripple at 120 Hz.

Since the LED output light is a function of its forward current, any LED current ripple will result in an output light modulation (flicker). In this way, for a better insight about flicker in different frequencies, the measured LED current is evaluated through fast Fourier transformation and then the modulation index (Modulation(%)) is calculated. Figure 7 shows the driver Modulation(%) in comparison to the IEEE Std 1789-2015 limits. Experimental results are shown for three different LED current reference (1.15 A, 0.7 A and 0.250 A). It is worthy to mention that for frequency higher than 600 Hz and lower than 3 kHz, no significant harmonic content is noticed in the measured current, being omitted in Figure 7. As it can be seen, the ARC maintain the LED current ripple under the limits imposed by the related recommendation practices.

Figure 8 shows the LED current dynamic behavior when a 10 V DC voltage is added to steady-state bus voltage, changing its DC value from 390 V to 400 V. The bus voltage ripple was maintained in 42 V peak to peak. As it can be seen, after the transient period, the LED current returns to its reference.

#### 4.1 Final remarks

It is known from (Ioannou and Tsakalis, 1986) that for adaptive controllers guarantee a zero residual tracking errors it is required an input signal to have as many frequencies as possible to persistently excite the system, which makes the adaptive controller not usual for DC/DC converters. Nevertheless, evaluating the experimental results shown, it can be seen a stable operation over all the tested conditions with a negligible tracking error. In this way, it can be inferred the converter bus voltage ripple has frequencies that persistently excite the system, allowing the adaptive controller parametric variables to reach a stable solution. This condition enables the MRAC use in DC/DC converter.

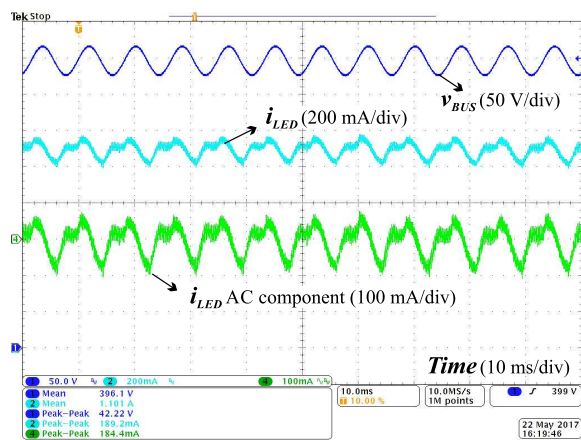


Figure 5 Bus voltage (CH1, 50 V/Div), LED current (CH2, 200 mA/Div) and AC component of the LED current (CH4, 100 mA/Div) under steady-state operation for the nominal output LED current (1.15 A).

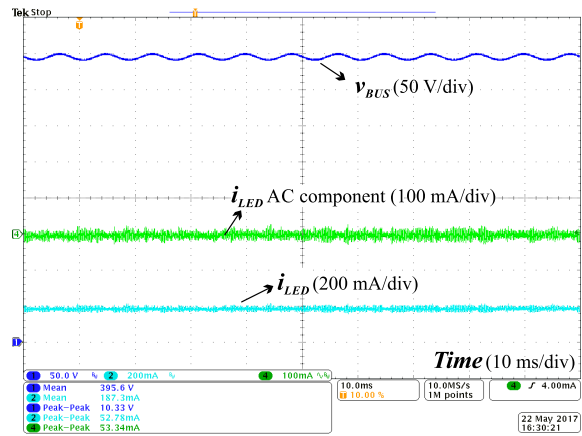


Figure 6 Bus voltage (CH1, 50 V/Div), LED current (CH2, 200 mA/Div) and AC component of the LED current (CH4, 100 mA/Div) under steady-state operation for the minimal output LED current (250 mA).

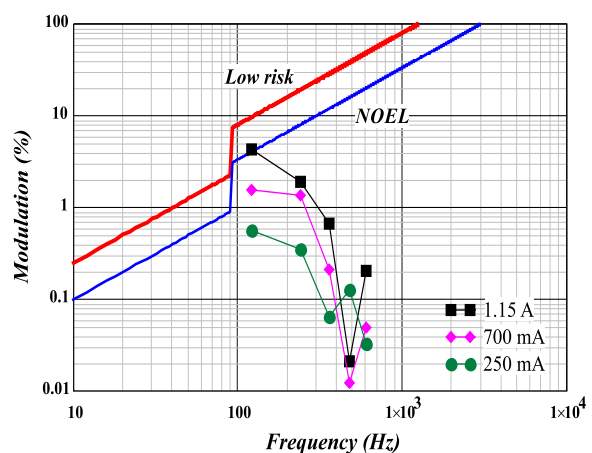


Figure 7 Low-risk level and No Observable Effect Level (NOEL) Modulation(%) analysis of the proposed driver.

## 5 CONCLUSION

This paper presented the model reference adaptive control (MRAC) applied to control the LLC LED driver. The MRAC is responsible to both control the average LED current and implement the active ripple compensation. Experimental results shows the feasibility of the MRAC applied in the LLC LED driver, which the average LED current was under control, as well, a reduced current ripple is noticed for all the tested conditions.

Due to the nature of the MRAC, the gain of the controller is automatically updated, providing a good performance for a wide operation area. To obtain a similar performance using a classical controller, for instance with an Integrator + Quasi-resonant (I+QR) controller, a set of different gains has to be provided to the control system. Therefore, based on the detected operating point, the controller uses the predefined gains. In this way, it becomes a challenging and hard task to design the proper gain as function of the operating point.

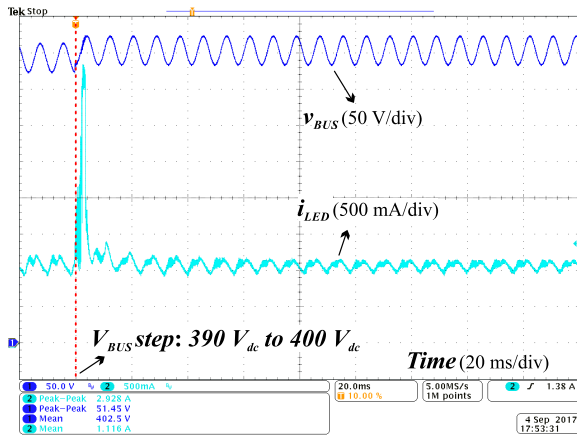


Figure 8 Bus voltage (CH1, 50 V/Div) and LED current (CH2, 500 mA/Div) for a bus voltage step from 390 Vdc to 400 Vdc.

### ACKNOWLEDGEMENT

The authors would like to thank for the financial support: the Coordination for the Improvement of Higher Education Personnel (CAPES), process number 23038.000776/2017-54; the National Council for Scientific and Technological Development (CNPq), through the process number 311911/2015-3, 409632/2016-3 and 465640/2014-1; and to the Research Support Foundation of the State of Rio Grande do Sul (FAPERGS) through CNPq under Grant FAPERGS 17/2551-0000517-1.

### References

- Almeida, P. S., Camponogara, D., Costa, M. A. D. and Alonso, J. M. (2015). Matching LED and Driver Life Spans, *IEEE Industrial Electronics Magazine* (June 2015): 36–47.
- Branas, C., Azcondo, F. J. and Alonso, J. M. (2013). Solid-state lighting: A system review, *IEEE Industrial Electronics Magazine* 7(4): 6–14.
- Chang, C. H., Chang, E. C., Cheng, C. A., Cheng, H. L. and Lin, S. C. (2012). Small Signal Modeling of LLC Resonant Converters Based on Extended Describing Function, *Computer, Consumer and Control (IS3C), 2012 International Symposium on* pp. 365–368.
- IEEE Power Electronics Society (2015). *IEEE Recommended Practices for Modulating Current in High-Brightness LEDs for Mitigating Health Risks to Viewers*.
- Ioannou, P. and Tsakalis, K. (1986). A robust direct adaptive controller, *IEEE Transactions on Automatic Control* 31(11): 1033–1043.
- Lin, R. L., Liu, S. Y., Lee, C. C. and Chang, Y. C. (2013). Taylor-series-expression-based equivalent circuit models of LED for analysis of LED driver system, *IEEE Transactions on Industry Applications* 49(4): 1854–1862.
- Ma, H., Yu, W., Zheng, C., Lai, J. S., Feng, Q. and Chen, B. Y. (2011). A universal-input high-power-factor PFC pre-regulator without electrolytic capacitor for PWM dimming LED lighting application, *IEEE Energy Conversion Congress and Exposition*.
- Massing, J. R., Stefanello, M., Grundling, H. A. and Pinheiro, H. (2012). Adaptive current control for grid-connected converters with LCL filter, *IEEE Transactions on Industrial Electronics* 59(12): 4681–4693.
- Menke, M. F., Seidel, Á. R. and Tambara, R. V. (2018). LLC LED Driver Small-Signal Modeling and Digital Control Design for Active Ripple Compensation, *IEEE Transactions on Industrial Electronics* NA.
- Schratz, M., Gupta, C., Struhs, T. J. and Gray, K. (2016). A New Way to See the Light: Improving Light Quality with Cost-Effective LED Technology, *IEEE Industry Applications Magazine* 22(4): 55–62.
- Soares, G. M., Almeida, P. S., Alonso, J. M. and Braga, H. A. (2017). Capacitance minimization in offline LED drivers using an active-ripple-compensation technique, *IEEE Transactions on Power Electronics* 32(4): 3022–3033.
- Texas Instruments (2014). Tiva TM4C1294NCPDT Microcontroller.
- Wang, Y., Gao, S., Guan, Y., Huang, J., Xu, D. and Wang, W. (2016). A Single-Stage LED Driver Based on Double LLC Resonant Tanks for Automobile Headlight With Digital Control, *IEEE Transactions on Transportation Electrification* 2(3): 357–368.
- Wu, H. (2011). *Multi-Channel Constant Current (MC3) LED Driver for Indoor LED Luminaries*, Master of science thesis, Faculty of the Virginia Polytechnic Institute.
- Yang, E. X., Lee, F. C. and Jovanovic, M. M. (1992). Small-signal modeling of LCC resonant converter, *Power Electronics Specialists Conference, 1992. PESC '92 Record., 23rd Annual IEEE* pp. 941–948 vol.2.